Environmental Science and Pollution Research (2023) 30:91929–91944
https://doi.org/10.1007/s11356-023-28837-7

RESEARCH ARTICLE

Hydrochemistry and strontium isotope fingerprints of solute sources and CO_2 consumption in Changbai Mountain area, Northeast China

Yihan Li[1,2] · Jianmin Bian[1,2] · Peng Xu[1,2,3] · Xiaoqing Sun[1,2] · Wenhao Sun[1,2]

Received: 3 February 2023 / Accepted: 13 July 2023 / Published online: 22 July 2023

Abstract

As one of the most representative forms of groundwater, mineral water provides a critical understanding of regional hydrogeochemical features and rock weathering processes. However, current studies have mostly focused on the quality of mineral water and have rarely addressed the weathering process during its formation. Therefore, a multi-tracer approach combines chemical parameters, major ions, selected trace elements, and $^{87}Sr/^{86}Sr$ ratios for mineral water samples in Changbai Mountain during 2020–2021. First, we determined the hydrogeochemical characteristics of different types of mineral water. Secondly, the water-rock interaction processes governing the water mineralization were described to fix the hydrogeochemical background. Thirdly, the chemical weathering rate was calculated. The total dissolved load generated by rock weathering was around 6.76 tons/km^2/year in the mineral water catchment area; 44.6% and 36.9% of the dissolved load were derived from silicate and carbonate weathering, respectively. The trace carbonates also played an important role in the overall rock weathering. Finally, after fully considering various influencing factors, we concluded that lithological characteristics and the soil environment rich in organic acids were the most important factors affecting rock weathering in the Changbai Mountain area. Overall, this study highlights the mineral water's role in the fluxes of CO_2 in local area and reveals possible influence of the unique ecological and geological environment on rock weathering in Changbai Mountain. It can provide a reference for the subsequent assessment of environmental stability for basalt areas and the possibility of sustainable water resources development.

Keywords Hydrochemistry · Strontium isotope · Water-rock interaction · CO_2 consumption · Changbai Mountain

Introduction

The chemical composition of mineral water is often a reflection of rock composition (Panno et al. 2022; van der Aa 2003). Different types of mineral water can be formed under the combination of various factors such as stratigraphic lithology, geological formations, groundwater circulation conditions, geothermal fields, and hydrogeochemical fields (Elena et al. 2020; Fillimonova et al. 2022; Lavrushin et al. 2018; Spence and Telmer, 2006). The formation processes of metasilicate mineral water, strontium mineral water, and carbonated water are mainly due to the control of water-rock interaction (Bian et al. 2022; Dinelli et al. 2010; Wang et al. 2021a; Yan et al. 2017). Therefore, mineral water formation process also reflects chemical weathering process of rocks.

Chemical weathering of crustal rocks is one of the main geological processes affecting the climate (Paytan et al. 2021) and chemical changes on the Earth's surface (Spence and Telmer, 2005) and is also the main process of continental CO_2 consumption (Fan et al. 2014). Silicate weathering is of great significance to long-term global climate regulation and the maintenance of the long-term habitable natural environment of Earth (Kump et al. 2000; Maher and Chamberlain, 2014; Oliva et al. 2003). At geological

Responsible Editor: Christian Gagnon

✉ Jianmin Bian
bianjm@jlu.edu.cn

[1] Key Laboratory of Groundwater Resources and Environment, Ministry of Education, College of New Energy and Environment, Jilin University, Changchun 130021, China

[2] College of New Energy and Environment, Jilin University, Changchun 130021, China

[3] State Key Laboratory of Simulation and Regulation of Water Cycle in River Basin, China Institute of Water Resources and Hydropower Research, Beijing 100038, China

timescales, silicate weathering through carbonation reactions is the main long-term sink of atmospheric CO_2 (Fan et al. 2014) and has long-term control over atmospheric CO_2 (Aloisi et al. 2006; Berner and Maasch, 1996; Jiang and Lee, 2019; Liu et al. 2011). Compared to other silicate minerals, basalt is more susceptible to erosion and has a faster dissolution rate, which is the main contributor to silicate rock weathering (Bluth and Kump, 1994).

Since the Pliocene, massive basaltic volcanic rocks have erupted in the Changbai Mountain area (Guo et al. 2014). The basalt groundwater system is characterized by well-developed pores and fissures, abundant groundwater resources, and excellent water quality. The Changbai Mountain area is one of the three major mineral water sources worldwide (Yan et al. 2016). Mineral water is the main form of groundwater in this area and one of the important sources of main rivers (Li et al. 2022). The geochemical behavior of the dissolved load is so important for the detailed study of terrestrial weathering that the influence of the mineral water formation process on it cannot be ignored. Therefore, it is necessary to understand rock weathering, evaluate CO_2 consumption rates, and determine the influencing factors in the weathering process.

Strontium isotopes are also widely used in hydrogeology to characterize weathering processes conditioned by water-rock interactions (Ettayfi et al. 2012; Negrel et al. 2003; Negrel and Pauwels, 2004; Negrel et al. 2018; Santoni et al. 2016; Shand et al. 2007; Wang et al. 2006). As Sr isotopes rarely fractionate in the water environment and the $^{87}Sr/^{86}Sr$ ratio signature of atmosphere input is always quickly replaced by the rock signatures, the $^{87}Sr/^{86}Sr$ ratios are more sensitive to water sources than other traditional hydrogeochemical analyses and are constrained by mineral and weathering processes (Bickle et al. 2003). Therefore, examining the $^{87}Sr/^{86}Sr$ ratios in groundwater systems is a powerful approach to understanding geochemical interactions. The amount of dissolved matter and CO_2 consumption associated with rock weathering can often be estimated using major elements of water (Dalai et al. 2003; Zhang et al. 2019). The chemical characteristics of natural water result from long-term interactions with the surrounding environment during the cycle (Carol et al. 2009; Toth 1999; Zhang et al. 2020), and its chemical composition records the history of water formation and migration (Vaughn and Fountain 2005). Quantity and charge conservation of matter are the theoretical bases of hydrochemistry research. By comparing and analyzing different compositions and using hydrochemistry statistics and water stoichiometry, it is possible to clarify the differences in hydrogeochemical processes (Wu and Wang 2014), determine the control mechanism of water body formation, and identify the source of ions and the formation processes of water chemistry (Bello et al. 2019; Gaillardet et al. 1999; Ryu et al. 2007). Combining Sr isotopes with hydrochemical analysis methods can effectively reveal the contribution and influencing factors of weathering in the process of solute formation (Deuerling et al. 2018; Shi et al. 2021).

This research focuses on the basalt area of Changbai Mountain (China). Mineral water is the main presentation of groundwater in this area, and it is also one of the main sources of local water supply as well as an important economic pillar. Sr isotopes and hydrochemistry indications have been widely used in rock weathering, but there is a relatively blank in research related to this area. Based on this, the main research objectives of this study are to (1) interpret the source and final element contributions of chemical weathering to Sr isotopic composition and dissolved ions; (2) quantify the chemical weathering and CO_2 consumption rate in the study area; and (3) explore the factors affecting the chemical weathering process. In this study, the source of the dissolved load of mineral water was analyzed using Sr isotope and hydrogeochemical methods, which will help to better understand the chemical weathering process of basalt mountains. It can also provide a reference for the study of water quality sustainability in the subsequent extraction of mineral water resources.

Materials and methods

Study area

The study area is located in the eastern part of the Jilin Province and the northern part of the Changbai Mountain (Fig. 1). It is a typical temperate continental mountain region with long winters and short summers. The Songhua River is the main river in this area and has many tributaries. Under the influence of volcanic tectonic movement, volcanic lava landforms comprising volcanic platforms, plateaus, and cones have a relatively wide development area, forming the basic geomorphic form in the study area (Yan et al. 2019). The terrain of the Tianchi area in Changbai Mountain gradually decreases from southeast to northwest. The east comprises a volcanic cone and volcanic lava platform, and the northwest gradually transitions to a landform dominated by medium and low mountains. Massive faults have formed the main tectonic pattern in the study area since the Cenozoic and the most important faults are along the northeast, northwest, and east–west directions (Zhao et al. 2019; Zhao and Yi 2021). The Changbai Mountain area belongs to the North China Plateau. The regional strata are distributed from the Archean to Cenozoic, and their development is relatively complete. The Longgang Group of the Archaeozoic is distributed in the northwest region of the study area, while the Jiapigou Group is distributed in the southwest region. Basalt was the main lithology of the study area and is mostly olivine basalt.

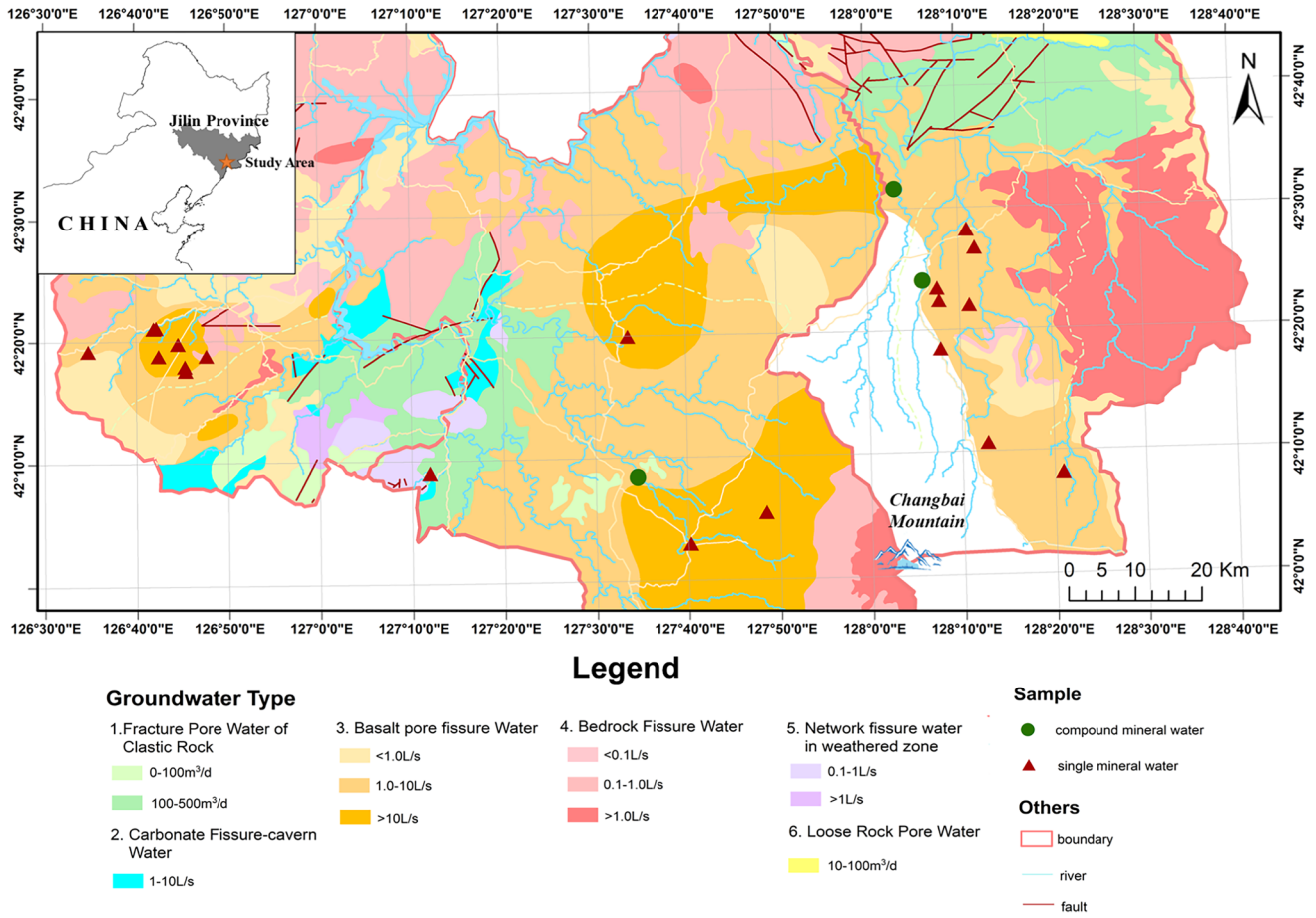

Fig. 1 Study area and sampling

Its distribution accounts for more than 50% of the study area, with an overall thickness of 500–1700 m (Yan et al. 2015). The mineral is mainly comprised of pyroxene, plagioclase, and olivine and contains a small amount of dolomite, calcite, and strontianite.

The complexity of the geological background leads to the diversity of groundwater types and different water-rich degrees in the entire region, and the distribution of groundwater has a certain regularity. According to conditions of groundwater occurrence, physical properties, and hydrological and hydraulic characteristics, groundwater can be divided into basalt pore fissure water, granite fissure water, carbonate fissure dissolved fissure water, and bedrock fissure water (Wang et al. 2021b; Yan et al. 2016).

The widespread distribution of basalt causes groundwater to become metasilicate-rich mineral water during runoff. The presence of faults and lush vegetation provides excellent migration and conservation conditions for the formation of high-quality mineral water. Mineral water is the main form of groundwater in the study area and is the main source of river water. It also has a certain impact on river water quality. The identification of solute sources is of great significance for the protection and utilization of water resources in the study area.

Sampling and chemical analysis

A total of 45 mineral water samples were collected for hydrochemical and isotope analyses from July 2020 to April 2021. The mineral springs in the study area are distributed near the rivers. The flow direction of rivers and groundwater is from south to north due to the existence of Changbai Mountain. Therefore, we collected mineral and surface water according to the flow direction and covered all types of springs (single and compound mineral water) in the study area. Polyethylene bottles (500 mL) were used to collect water samples. Subsequently, the bottles were sealed, stored at 4 °C, and transported to the laboratory for testing.

The chemical composition was measured at the Public Technology Service Center of the Northeast Institute of Geography and Agroecology, Chinese Academy of Sciences. The cations and SO_4^{2-} were measured using an inductively coupled plasma emission spectrometer (ICP-7500, Agilent Technologies Inc., Palo Alto, CA, USA), and the detection

limit was less than 10 μg/L. The other anions were measured by titration, and the detection limit was 1 mg/L. The detection accuracy was found to be 5%. Anion balance verification was conducted to ensure that the error range of credibility was ±10%. The validity of the chemical analysis was checked by calculating the ionic balance error and the analysis was rejected when the ionic balance error was greater than 5%.

Sr isotopes were measured using a Phoenix Hot Surface Ionization Mass Spectrometer 9444 at the Analysis and Testing Research Center of the Beijing Institute of Geology of the Nuclear Industry. The detection basis of Sr isotopes was GB/T 17672-1999 and the detection error was 2σ.

Data analysis

Owing to a large number of chemical variables for each sample, regional hydrogeochemical research has become a multi-variable problem. Therefore, multivariate statistical analysis is used to quantify the different types of water samples and determine the correlation between chemical parameters and groundwater samples (Cloutier et al. 2008). This study first used the Statistical Package for the Social Sciences (SPSS) to conduct statistical and correlation analyses on the hydrochemistry data, and Aquachem was used to draw a Piper diagram to explain the hydrochemistry characteristics. Hierarchical clustering analysis (HCA) was used to classify water samples according to their chemical parameters (Chai et al. 2020; Cloutier 2004; Lambrakis et al. 2004). This helps to effectively understand the distribution characteristics of the hydrochemistry implicit in the dataset. The dendrogram can identify the distance relationship between clusters, thus providing a basis for further effective use of the hydrochemistry data.

Based on the HCA results, the stoichiometric ratios of different components were selected using the hydrochemistry stoichiometry method, and the reactions and equilibrium processes of the chemical elements in the solute were studied (Han and Liu, 2004). Combined with an endmember comparison of Sr isotopes, we identified the source material for rock weathering. Based on the above methods, we obtained the traceability results of rock weathering and used a forward model to quantitatively assess the contribution of different endmembers to the solute (Li et al. 2019; Moon et al. 2007; Zhang et al. 2021).

The forward model calculates the source of the dissolved load in water through five basic cation sources (precipitation, anthropogenic input, evaporite, silicate, and carbonate). The mass balance equation is expressed as follows (Roy et al. 1999):

$$[\mathrm{X}]\text{mineral water} = [\mathrm{X}]\text{atmosphere} + [\mathrm{X}]\text{carbonate} + [\mathrm{X}]\text{silicate} + [\mathrm{X}]\text{evaporation} + [\mathrm{X}]\text{anthropogenic} \quad (1)$$

where X means any element in water. Mineral springs in the Changbai Mountain area are all located in the nature reserve. Therefore, there is no impact of anthropogenic activities. $[X]$anthropogenic can be considered as zero.

After obtaining the contribution of different rocks to the dissolution load, the sum of cations can be used to estimate the weathering and CO_2 consumption rates of different rocks. The contributions of silicate weathering, carbonate weathering, and evaporite dissolution to total dissolved solids (TDSs) were calculated using the following equation (Wu et al. 2013):

$$\begin{gathered}[TDS]_{sili} = [Ca]_{sili} + [Na]_{sili} + [K]_{sili} + \left[Mg\right]_{sili} + \left[SiO_2\right] \\ [TDS]_{carb} = [Ca]_{carb} + \left[Mg\right]_{carb} + \tfrac{1}{2}\left[HCO_3\right] \\ [TDS]_{evap} = [Ca]_{evap} + [Na]_{evap} + [Cl]_{evap} + \left[Mg\right]_{evap} + \left[SO_4\right]_{evap}\end{gathered} \quad (2)$$

The rate of CO_2 consumption during silicate and carbonate weathering can be determined using the following equation (Moon et al. 2007):

$$\begin{gathered}\left[\phi CO_2\right]_{sili} = \phi\left(2Ca_{sili} + Na_{sili} + K_{sili} + 2Mg_{sili}\right) \\ \left[\phi CO_2\right]_{carb} = \phi\left(Ca_{carb} + Mg_{carb}\right)\end{gathered} \quad (3)$$

where ϕ is CO_2 consumption rate and sili, carb, and evap represent the silicate, carbonate, and evaporate endmembers, respectively.

Results

Distinguishing major ions in mineral water

According to the requirements of the "National Standard for Food Safety-Drinking Natural Mineral Water" (GB8537-2018, China), mineral water in this area can be divided into two types (Table 1): metasilicate mineral water, strontium mineral water (both are single mineral water), and compound mineral water. The chemical characteristics of the mineral water in the study area are presented in Table 2. HCO_3^- has an absolute advantage in anions for mineral water. Ca^{2+} has a slight advantage in cations of single mineral water, whereas the content of cations in compound mineral water is similar.

Single mineral water has weak alkalinity and low TDS content. Compound mineral water is subacidic, and the content of each component is significantly higher than that of single mineral water. This may be attributed to the presence of a large amount of free CO_2 which promotes other components of the solute.

A correlation analysis of ions in single and compound mineral water was conducted, and the results are shown in Fig. 2.

Table 1 Classification criteria for mineral water in China

Type of mineral water		Component content			
		$H_2SiO_3 > 25$ mg/L	$Sr^{2+} > 0.25$ mg/L	TDS > 1000 mg/L	Free $CO_2 > 250$ mg/L
Single mineral water	Metasilicate mineral water	√			
	Strontium mineral water		√		
Compound mineral water				√	√

There were certain differences in the ion correlations between the single mineral water and compound mineral water, as shown in Fig. 2. In compound mineral water, the relationship between TDS and the other components was more obvious. The TDS of single mineral water was mainly affected by high Ca^{2+} and HCO_3^-. H_2SiO_3 was affected by other components in two different types of mineral water in contrasting ways, but the relationship between pH and Ca^{2+} was the most significant. Additionally, there was a positive correlation between free CO_2 and other compounds in compound mineral water, indicating that the existence of free CO_2 had a promoting effect on the dissolution of other components; thus, the overall content of each component in compound mineral water was larger than that in single mineral water.

A Piper diagram was drawn using the AqQA software to analyze the hydrochemical types of mineral water, as shown in Fig. 3. The Piper diagram classifies mineral water into HCO_3-Mg, HCO_3-Ca, and HCO_3-Na types, wherein HCO_3-Mg was the dominant type. Similarly, different single mineral water samples also showed certain differences. The Ca^{2+} content in the strontium mineral water was higher than that in the metasilicate mineral water.

Clustering analysis of major elements

Chemical variables such as the dissolved H_2SiO_3, Sr^{2+}, free CO_2, and the pH of water were integrated. HCA was used to characterize the categories of the water samples, and the results are shown in Fig. 4.

HCA classifies individuals to reduce them to a small number of water sample groups with similar lithological origins (Cloutier et al. 2008). The number of clusters depended on the linkage distance threshold. When the threshold value was the largest, the difference between the different groups was the largest. Mineral water was mainly divided into single mineral water and compound mineral water. This result complies with the mineral water classification standards and was consistent with the hydrochemical analysis. When the threshold was fixed at three, five clusters could be distinguished according to the chemical composition of the mineral water. Single mineral water was divided into two categories, and compound mineral water was divided into three categories, indicating different regions and geological characteristics. Among the single-type mineral springs, most metasilicate mineral springs were located in the basalt distribution area, and the strontium mineral spring was located at the junction of clastic rocks and carbonate salts with the developed river networks. Three complex mineral springs were located at different locations in the study area. Subtle lithological differences and different recharge types may exist, leading to different groups.

When the connection distance between subgroups in the same group was 1, the metasilicate mineral water was known to have a certain similarity. Therefore, the comparisons between similar subgroups were not significant. Notably, the Schoeller diagram (Fig. 5) shows that the connecting line segments of adjacent ions in the metasilicate mineral water are almost parallel, indicating that the supply source of the water was consistent and the formation process was similar. The ionic connections between the metasilicate and compound mineral water were considerably different, and a difference also existed between metasilicate and Sr mineral water. However, the trend of the ion connection lines between compound mineral water was roughly the same. Our previous study (Li et al. 2022) found that rainwater was the main recharge of mineral water. This suggested a similarity in the recharge mechanism of different mineral springs. But the compound mineral spring was affected by deep underground circulation, volcanic activity, and soil leaching, and the geological lithology surrounding the strontium mineral water was carbonate, whereas this of the other types of mineral springs was basalt. These led to variability in ions. Therefore, we mainly divided mineral springs into metasilicate, strontium, and compound.

Strontium isotope composition

The $^{87}Sr/^{86}Sr$ and Sr^{2+} concentrations of the mineral water in the study area are presented in Table 2. Except for the J-5, the ratio of $^{87}Sr/^{86}Sr$ was between 0.707 and 0.710 for single mineral water. The $^{87}Sr/^{86}Sr$ ratio of the compound mineral

Table 2 Main chemical characteristics of the water samples

Spring type	Sample point	pH	Ca^{2+} mg/L	Mg^{2+}	Na^{+}	K^{+}	HCO_3^{-}	SO_4^{2-}	Cl^{-}	H_2SiO_3	Sr^{2+}	Free CO_2	TDS	$^{87}Sr/^{86}Sr$	Std err
Single mineral water	J-1	7.42	11.62	8.52	8.57	9.93	89.47	4.71	9.85	28.67	0.06	10.56	131.90	0.708305	0.000013
	J-2	7.42	17.10	13.35	10.63	4.64	127.19	7.76	9.12	35.07	0.11	8.36	171.59	0.708534	0.000014
	J-3	7.60	10.47	7.87	7.38	3.55	73.34	8.28	12.43	30.18	0.06	4.84	127.00	0.707095	0.000021
	J-4	7.56	11.39	9.24	9.13	4.36	97.92	6.89	16.33	36.92	0.06	7.92	186.00	0.709897	0.000017
	J-5	7.43	16.02	7.34	5.25	3.06	73.20	11.93	9.94	36.90	0.09	4.40	77.00	0.713356	0.000016
	J-6	7.85	11.45	8.97	7.96	4.65	89.01	7.96	6.82	42.36	0.07	4.40	134.00	–	–
	J-7	7.70	10.29	7.56	6.51	3.68	76.71	6.91	8.80	35.30	0.10	2.20	121.00	–	–
	J-8	7.06	37.96	23.91	21.18	5.29	230.05	7.54	11.88	37.11	0.19	17.42	307.23	0.709166	0.000016
	J-9	7.55	28.20	22.85	8.79	4.25	177.56	17.18	5.68	42.8	–	–	311.57		
	F-1	7.35	5.76	2.32	3.84	1.74	32.05	4.09	9.44	23.20	0.04	5.28	34.50	0.707702	0.000020
	F-2	7.44	2.90	0.99	6.36	1.96	21.08	3.01	7.10	33.72	0.02	2.29	75.00	–	–
	F-3	7.25	5.90	3.79	12.25	2.64	61.49	2.44	9.94	40.19	0.02	2.73	96.00	–	–
	A-1	7.14	4.52	3.05	6.01	3.01	37.79	4.01	6.69	47.32	0.03	4.62	77.43	0.707358	0.000019
	A-2	7.27	6.24	2.41	9.58	2.91	51.33	4.08	3.11	55.88	–	5.56	122.11	–	–
	A-3	7.11	4.93	3.94	9.29	3.25	54.05	2.49	7.46	50.26	0.03	8.19	100.79	–	–
	A-4	7.28	5.72	4.65	7.59	3.07	56.97	3.18	7.10	51.60	0.03	8.52	99.37	0.707785	0.000021
	A-5	7.15	5.49	5.35	6.57	3.28	55.63	4.46	11.36	58.11	0.18	84.91	50.00	–	–
	A-6	7.24	5.00	4.27	7.13	3.07	46.26	6.85	11.08	44.40	0.03	7.04	66.00	–	–
	A-7	6.87	5.32	3.72	6.84	3.19	45.40	3.66	9.18	47.91	0.04	11.55	70.08	0.707180	0.000015
	A-8	7.12	5.68	4.27	9.37	3.30	60.53	2.72	3.35	55.90	–	6.94	132.86	–	–
	FS-1	7.67	61.98	11.11	2.11	1.43	185.04	43.92	11.72	12.98	0.42	8.80	204.50	0.707159	0.000011
Min		6.87	2.90	0.99	2.11	1.43	21.08	2.44	3.11	12.98	0.02	2.20	34.50	–	–
Max		7.85	61.98	23.91	21.18	9.93	230.05	43.92	16.33	58.11	0.42	84.91	311.57	–	–
Mean		7.36	13.04	7.59	8.21	3.63	82.96	7.81	8.97	40.32	0.09	10.83	128.38	–	–
Compound mineral water	FC-1	6.63	160.41	132.19	218.77	25.01	1782.84	49.54	40.47	35.08	435.38	2.00	1842.50	0.709165	0.000015
	AC-1	6.26	89.24	140.14	132.65	11.10	1290.47	1.65	21.06	103.50	326.19	0.54	1257.60	0.710770	0.000016
	AC-2	6.64	167.04	79.69	46.19	7.13	1046.76	6.71	13.41	52.55	252.66	0.42	1024.80	0.712571	0.000016
Min		6.26	89.24	79.69	46.19	7.13	1046.76	1.65	13.41	35.08	252.66	0.42	1024.80	–	–
Max		6.64	167.04	140.14	218.77	25.01	1782.84	49.54	40.47	103.50	435.38	2.00	1842.50	–	–
Mean		6.51	138.89	117.34	132.54	14.41	1373.35	19.30	24.98	63.71	338.08	0.99	1374.97	–	–

The hydrochemistry data in the table is an average of data for 2020–2021

"–" represents not detected or not measured

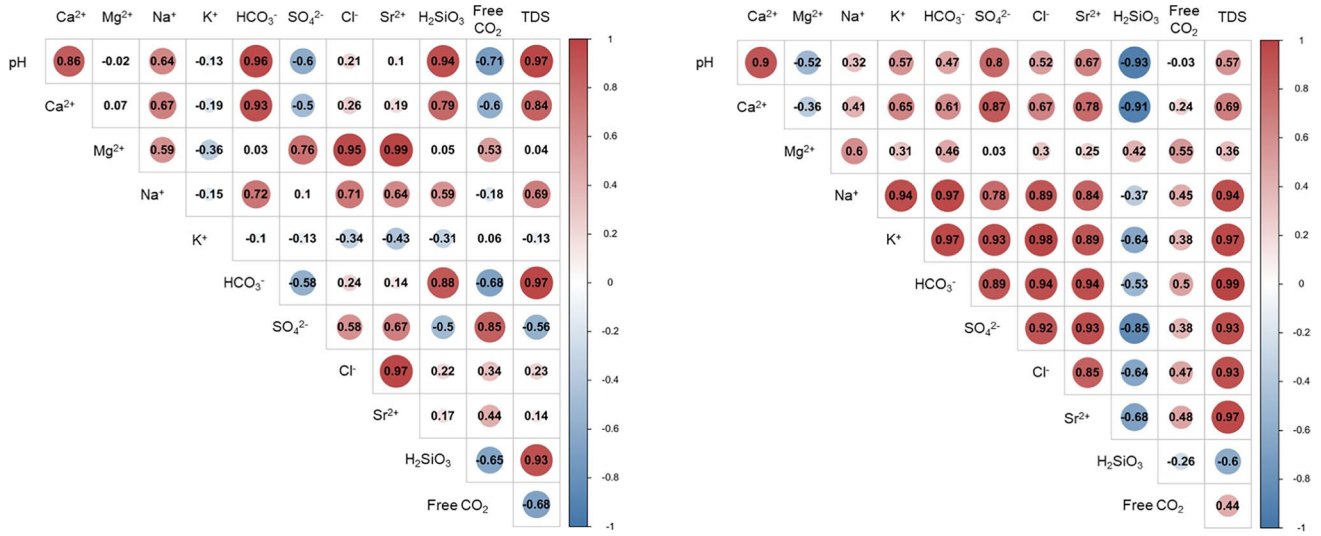

(a) Single mineral water **(b) Compound mineral water**

Fig. 2 Correlation analysis (red dots represent the positive correlation, and blue dots represent the negative correlation. The larger the dot, the greater the correlation)

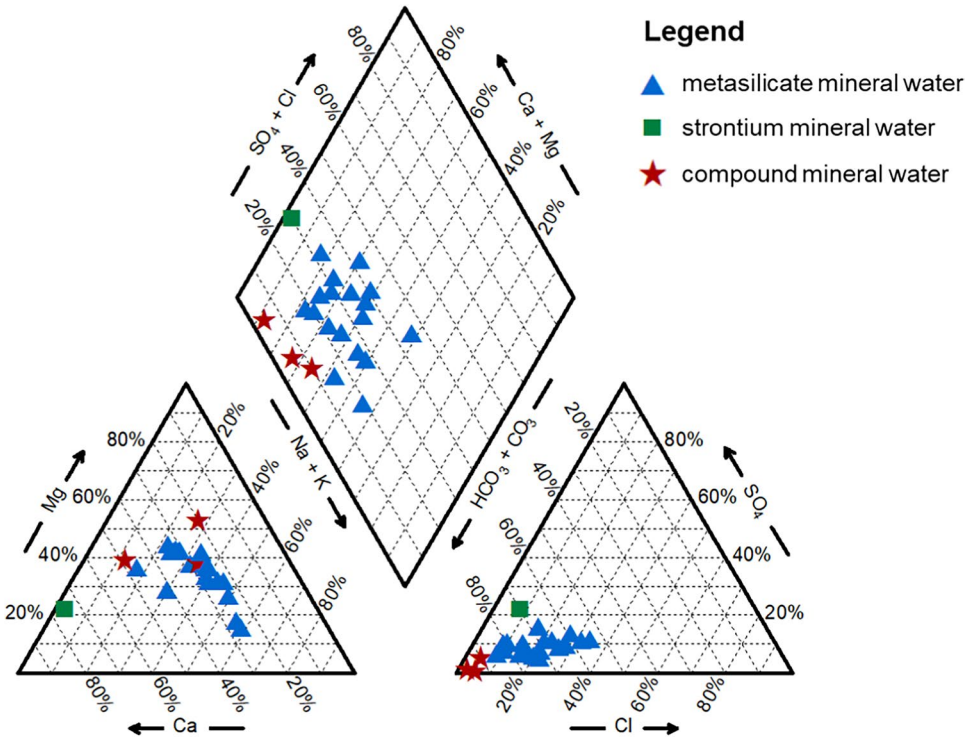

Fig. 3 Piper diagram of water samples

water was slightly higher, ranging from 0.709 to 0.713. This narrow range of Sr isotopic compositions indicates that there is little regional variation in the $^{87}Sr/^{86}Sr$ content. The $^{87}Sr/^{86}Sr$ of basalt in the study area ranges from 0.703 to 0.706. The ratios of water were all higher than the local basalt isotope ratio, indicating the influence of other rocks.

Strontium can be derived from carbonate, sulfate, and silicate mineral weathering. Na^+ is mainly from silicate, while Ca^{2+} is mainly from carbonate. Therefore, Sr/Na, Ca/Na, and $^{87}Sr/^{86}Sr$ ratios can be used as effective parameters to distinguish the rock species that release Sr from groundwater. The relationship between them can indicate the mixing process

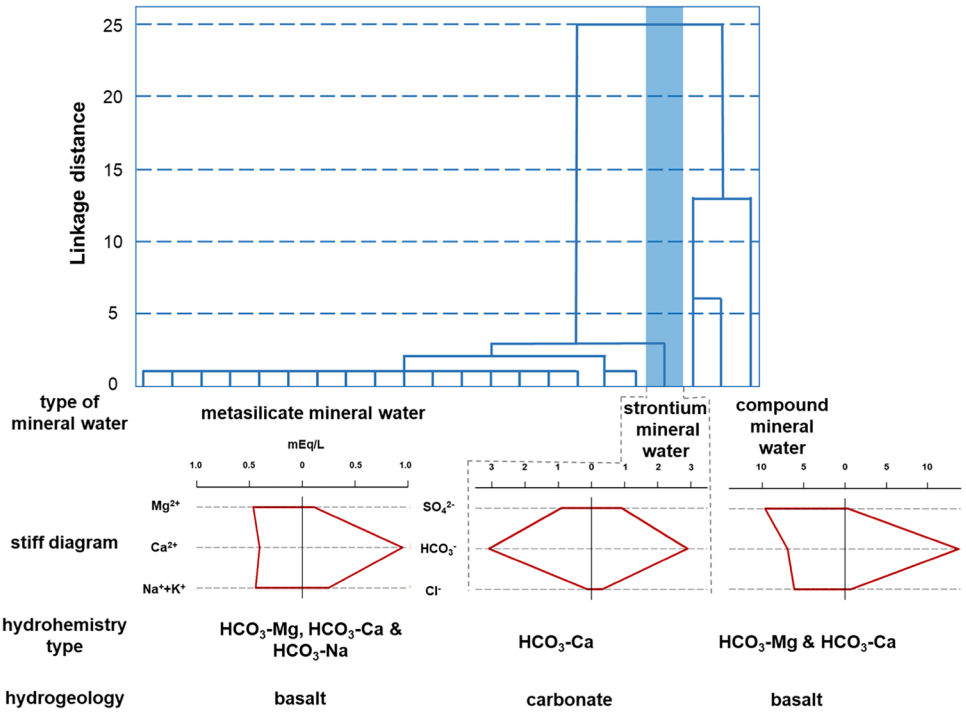

Fig. 4 Comparison of the chemical patterns using hierarchical clustering analysis of the chemical composition of mineral water

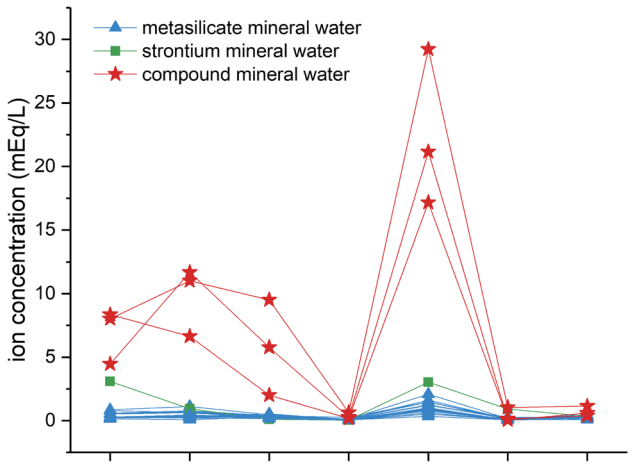

Fig. 5 Schoeller diagram of water samples

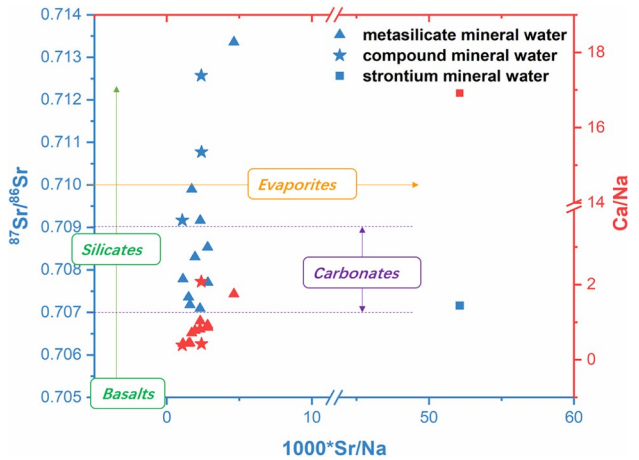

Fig. 6 The comparison of different ratios

of carbonate (with high Sr/Na and Ca/Na) with silicate or evaporative salts (both with low Sr/Na and Ca/Na) (Gaillardet et al. 1999). A comparison between these three ratios is shown in Fig. 6.

The $^{87}Sr/^{86}Sr$ ratios of most springs in the study area were concentrated in the carbonate zone. For silicates, however, the Sr isotopic composition primarily depended on age; therefore, it was expected to be more dispersed, ranging from 0.705 to 0.730. Additionally, Sr/Na and Ca/Na in all springs except strontium mineral water were relatively low, and the distribution was relatively concentrated; therefore, silicate was still dominant. However, the strontium mineral water showed a completely different distribution. The spring point (FS-1) had a high Sr^{2+} content (0.42 mg/L) and a high Sr/Na to Ca/Na ratio, indicating that it was mainly controlled by carbonate.

The ionic origin was further identified by the significant differences in the concentration ratios of Mg^{2+}/Na^+, Ca^{2+}/Na^+, and HCO_3^-/Na^+ produced by the weathering of carbonates, silicates, and evaporates (Wu and Wang 2014). Based on Gaillardet et al. (1999) and Wu et al. (2018), we obtained the endmember eigenvalues of mineral weathering in carbonates, silicates, and evaporates for comparison (Fig. 7). Mineral water samples were mostly distributed near the end

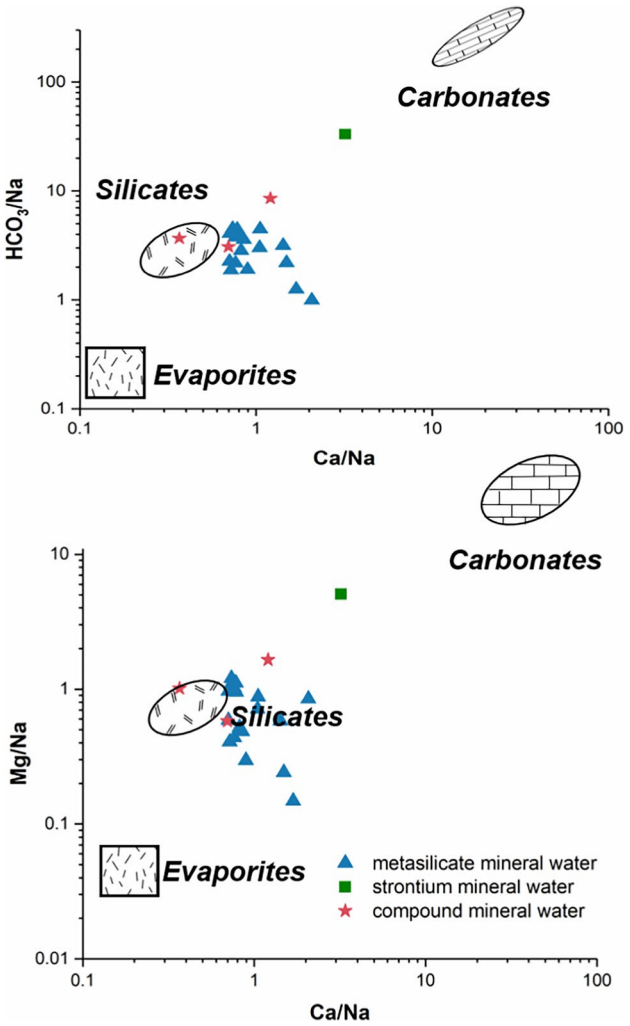

Fig. 7 Mixing diagrams using Na-normalized molar ratios in the dissolved phase of water samples

of the weathering and hydrolysis of silicate, indicating that they play a controlling role in the hydrogeochemical characteristics. In particular, carbonate minerals also contribute to strontium mineral water to some extent.

Discussion

Sources of dissolved elements and possible weathering processes

Gibbs diagrams (Gibbs 1970) can reflect the main processes of precipitation, rock weathering, or evaporation, and quickly and qualitatively describe water ions' sources. Gibbs diagrams and modified Gibbs diagrams of the mineral water samples (Amiri and Berndtsson 2020; Marandi and Shand 2018) are shown in Fig. 8.

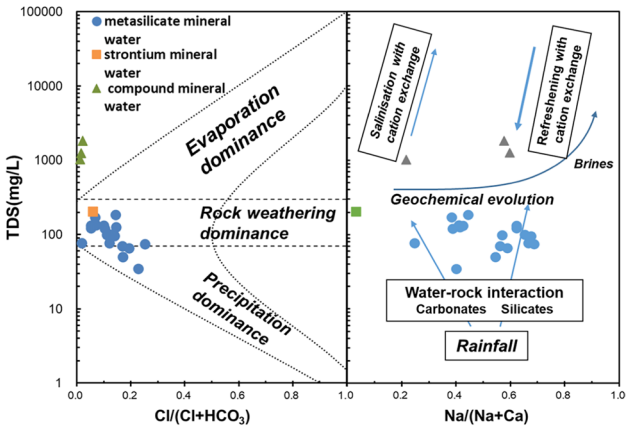

Fig. 8 Gibbs diagrams of water samples

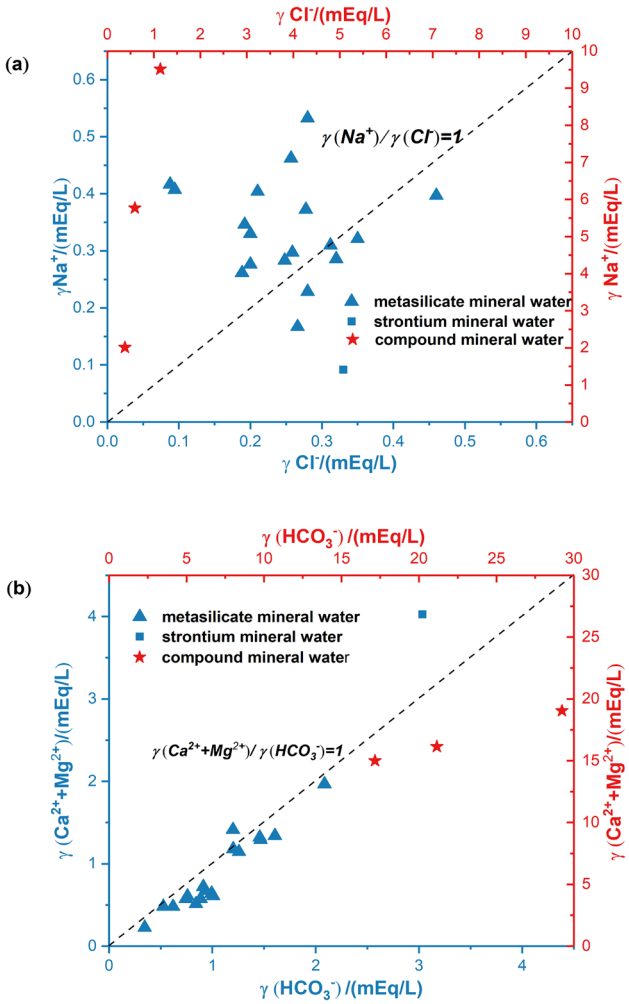

Fig. 9 Relationship between different ions in mineral water

According to the Gibbs diagram, rock weathering was the main ion source. However, an ion exchange effect also occurred; thus, the ion formation process can be further identified by the water stoichiometry method. The ion equivalence ratio was used to characterize the degree of ion enrichment in water (Fig. 9) to explore the genetic mechanism.

The compound mineral water and most metasilicate mineral waters are above the $\gamma(Na^+)/\gamma Cl^- = 1$ line (Fig. 9a), indicating the existence of excess Na^+ and that the contribution of marine aerosol input from the atmosphere was low. They require other rocks to dissolve to produce HCO_3^- or SO_4^{2-} to balance the excess Na^+. From the correlation analysis, the relationship between Na^+ and Cl^-, as well as between Ca^{2+} and SO_4^{2-} in single mineral water, was not obvious, implying that the dissolution of salt rock and gypsum was less. The strontium mineral water and a few metasilicate mineral waters fall below the $\gamma(Na^+)/\gamma Cl^- = 1$ line, indicating that the excess Cl^- needs to be balanced by Na^+ or K^+ derived from sources other than the dissolution of salt rocks and the recharge by atmospheric precipitation.

Figure 9b shows that all compound and metasilicate mineral water points fall near or slightly below $\gamma(Ca^{2+} + Mg^{2+})/\gamma(HCO_3^-) = 1$, indicating that the content of HCO_3^- was greater than the sum of Ca^{2+} and Mg^{2+}. The excess Na^+ in Fig. 9a can be balanced by HCO_3^-. The strontium-type mineral water falls above $\gamma(Ca^{2+} + Mg^{2+})/\gamma(HCO_3^-) = 1$, indicating an additional source of carbonate weathering that balanced the excess Ca^{2+} and Mg^{2+}. The HCO_3^- produced by CO_2 dissolved in water can dissolve carbonate minerals, but the atmospheric input of SO_2, H_2SO_4 formed by sulfide oxidation, and H_2SO_4 produced by gypsum dissolution can also dissolve the carbonate minerals (Han and Liu 2004), and the process can be expressed by the following equation:

$$3Ca_xMg_{1-x}CO_3 + H_2CO_3 + H_2SO_4 = 3xCa^{2+} + 3(1-x)Mg^{2+} + 4HCO_{3-} + SO_4^{2-}$$

This process also explains why SO_4^{2-} in strontium mineral water far exceeded that in other mineral waters under the main control of carbonate.

The ion exchange process reflected in the Gibbs diagram can be explained by calculating the chlor-alkali index and is further determined by the ion ratio $\gamma(Na^+ - Cl^-) + \gamma((Ca^{2+} + Mg^{2+}) - (HCO_3^- + SO_4^{2-}))$, as shown in Fig. 10. The chlor-alkali index was calculated as follows:

$$CAI - I = \frac{Cl - (Na + K)}{Cl}$$

$$CAI - II = \frac{Cl - (Na + K)}{HCO_3 + SO_4 + CO_3 + NO_3}$$

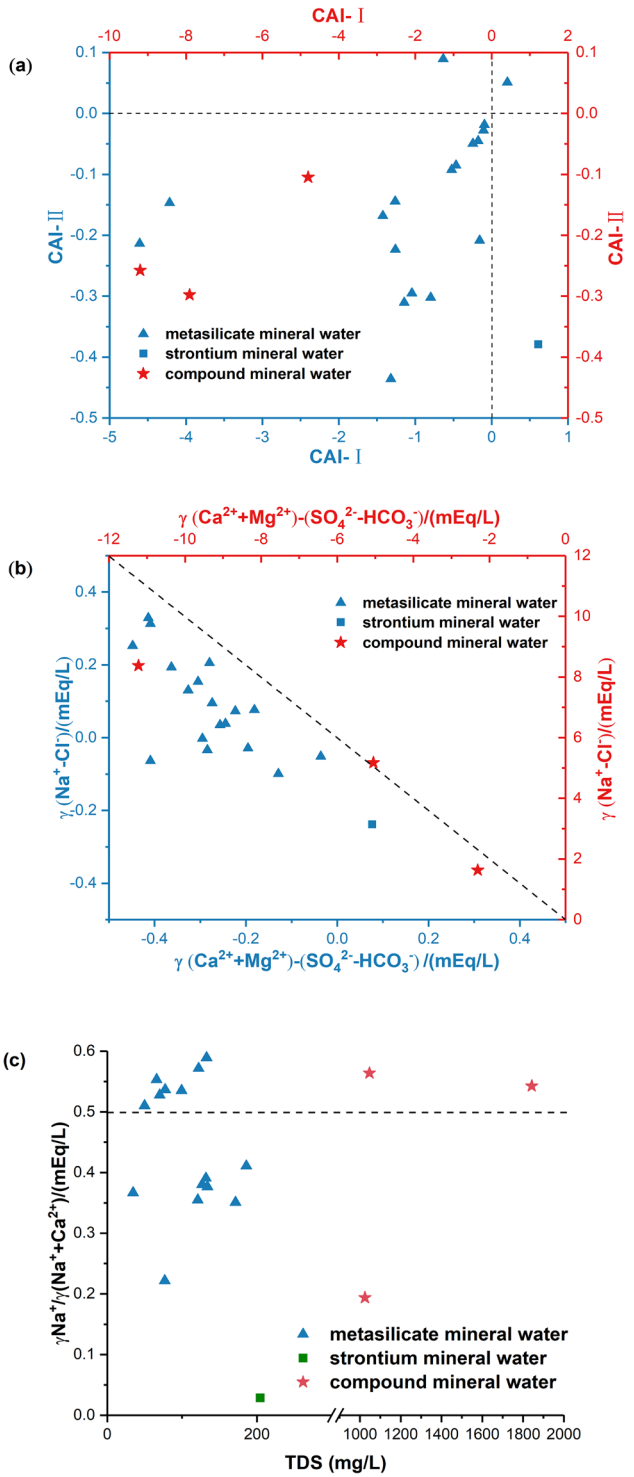

Fig. 10 Analysis of the ion exchange process

Figure 10b shows that all the water samples are distributed below the −1 line. The chlor-alkali index of compound mineral water and most metasilicate mineral water was less than 0. This indicated that an alkali exchange reaction occurred

and Na^+ was released into the water, which explains the existence of excess Na^+. During the cation exchange process, 2 mmol/L Na^+ was released due to the exchange of 1 mmol/L Ca^{2+}, and the masses of 1 mmol/L Ca^{2+} (40 mg/L) and 2 mmol/L Na^+ (46 mg/L) were almost equal, resulting in no significant change in the TDS value (Fig. 10c). The cation-exchange process is expressed as follows:

$$Ca^{2+} + Na_2 - X = 2Na^+ + Ca\text{–}X$$

where X is the cation exchange site.

Contribution of different chemical weathering

The comparison of various endmembers (Figs. 6 and 7) and the ion stoichiometry (Fig. 9) clearly show that mineral water was mainly controlled by two endmembers, silicate and carbonate. The mineral water in the study area was located in the nature reserve, which was less affected by anthropogenic activities, and there was no evaporative salt outcrop. Therefore, silicate and carbonate endmembers were selected in the quantitative calculation of the contribution of endmembers to Sr isotopes, and the calculation formula is as follows:

$$\left(\frac{^{87}Sr}{^{86}Sr}\right)_{sample} = C_{sili} \times \left(\frac{^{87}Sr}{^{86}Sr}\right)_{sili} + C_{carb} \times \left(\frac{^{87}Sr}{^{86}Sr}\right)_{carb}$$

$$C_{evap} + C_{sili} + C_{carb} = 1$$

where C represents the contribution rate of different endmembers. The values of each endmember are derived from Gaillardet et al. (1999), Ma et al. (2015), and Zhou et al. (1998). The results are presented in Table 3.

The above calculation results indicate that even for metasilicate and compound mineral water dominated by silicate, the contribution of carbonate to Sr isotopes was much greater than that of silicate. Notably, the dissolution flux of strontium and calcium can be controlled even with low carbonate mineral abundance (Blum et al. 1998; Clow et al. 1997; Horton et al. 1999; Santoni et al. 2016) due to the higher weathering rate of carbonate rocks (Blum et al. 1998; Clow et al. 1997; Horton et al. 1999; Santoni et al. 2016). This is especially true in basalts where trace carbonate rocks tend to contribute significantly to weathering in a more important position (Zeng and Liu 2017).

Table 3 Contribution of different endmembers

Endmembers	Contribution (%)		
	Compound mineral water	Metasilicate mineral water	Strontium mineral water
Silicate	33.5%	27.5%	41.2%
Carbonate	66.5%	72.5%	58.3%

Silicate and carbonate weathering reactions indirectly consume CO_2, and basaltic minerals undergo rapid dissolution. The basalt weathering rate controlling the atmospheric CO_2 concentration has been crucial for a long time. Research on the CO_2 weathering feedback hypothesis has a certain significance, and springs in the study area supply up to 60% of CO_2 in rivers (Li et al. 2022). This process also affected the change of solutes in rivers, especially the conversion of atmospheric CO_2 to bicarbonate, which can affect the precipitation and deposition of carbonate in the ocean in the long run (Dessert et al. 2003). Therefore, based on the differentiation of source rocks, we calculated the rock weathering rate and CO_2 consumption using the mass balance of the dissolved load in the water.

In the process of estimating the atmospheric contribution, conservative Cl^- was selected to calculate the contribution of atmospheric solutes to water, while the remaining Cl^- was derived from evaporation. We assumed that K^+ originated from silicate weathering, whereas Na^+ originated from silicate weathering and evaporation. The silicate weathering inputs of Ca^{2+} and Mg^{2+} were then estimated using single lithological ratios within the study area. For each element, the mass balance equation can be written based on Eq. (1), and the assumptions were discussed above.

$$[Cl] = [Cl]_{evap} + [Cl]_{prep}$$

$$[SO_4] = [SO_4]_{evap} + [SO_4]_{prep}$$

$$[K] = [K]_{sili} + [K]_{prep}$$

$$[Na] = [Na]_{sili} + [Na]_{evap} + [Na]_{prep}$$

$$[Ca] = [Ca]_{sili} + [Ca]_{carb} + [Ca]_{evap} + [Ca]_{prep}$$

$$[Mg] = [Mg]_{sili} + [Mg]_{carb} + [Mg]_{prep}$$

where (Ca/Na)sili = 0.2 and (Mg/K)sili = 0.5. The weathering and CO_2 consumption rates were calculated using Eqs. (2) and (3), respectively.

The total dissolved load generated by rock weathering was 6.76 tons/km^2/year, of which 44.6% and 36.9% of the dissolved load were derived from silicate and carbonate weathering, respectively, and the total CO_2 consumption rate was 1.44×10^{10} mol/year. The consumption rates of silicate and carbonate were 8.4×10^9 mol/year and 6.02×10^9 mol/year, respectively. For Sr mineral water dominated by carbonate rocks, the weathering and CO_2 consumption

rates of carbonates were considerably greater than those of silicate during its formation. For metasilicate and compound mineral water distributed among basalts, the weathering and CO_2 consumption rates of silicate were slightly higher than those of carbonate, but the difference was considerably small compared to the distribution range of the two rocks. For compound mineral water, owing to the existence of CO_2, the weathering of rocks was accelerated, resulting in increased CO_2 consumption. Therefore, the CO_2 consumption rates of silicate and carbonate did not differ significantly. This further verifies the key role of trace carbonates in the basalt weathering process.

Factors controlling the rock weathering rates

In the process of rock chemical weathering, water, acid, air, and other media play important roles in the transformation of fresh minerals into dissolved and secondary minerals. These media also change due to regional differences in climate, lithology, geological structure, etc., forming a variety of factors that control rock weathering (Buggle et al. 2011).

Based on the weathering mechanism, chemical weathering can be divided into supply- and power-limited types. Although the dynamic-limited type often occurs in tectonically active alpine regions, it is significantly limited by the climate (Dixon et al. 2012; Gabet and Mudd 2009; Riebe et al. 2017). Conversely, supply-limited chemical weathering is mainly controlled by the rate of fresh material supply (physical denudation) (Riebe et al. 2004), enhanced tectonic activity, or terrain slope. In general, the factors affecting the rock weathering process can be analyzed from external and internal aspects.

For internal factors, the rock structure and mineral composition are important for affecting chemical weathering. The rocks in the study area mainly comprise basalt, which lacks a crystal structure and is easily weathered (Meybeck 1987; Suchet and Probst 1995; Sun et al. 2019; Tao et al. 2011). The minerals comprising the basalt in the study area are mainly olivine and pyroxene. Under the same conditions, these two minerals have a higher weathering order than other silicate minerals (Fu et al. 2022; Nesbitt et al. 1996; Wimpenny et al. 2014), which facilitates rock weathering. Clay minerals, as typical products of weathering, also have an indicative function to weathering intensity (Fu et al. 2022). The dissolution of plagioclase produces Al^{3+} and H_2SiO_3, which continue to react and form kaolinite and montmorillonite, indicating that the rock is leached and moderately chemical weathered (Garzanti et al. 2013; Garzanti et al. 2014; Pang et al. 2018).

For external factors, environmental factors play an important role in weathering. The main sources of mineral water in the study area are atmospheric precipitation and alpine snowmelt, which provide abundant water sources

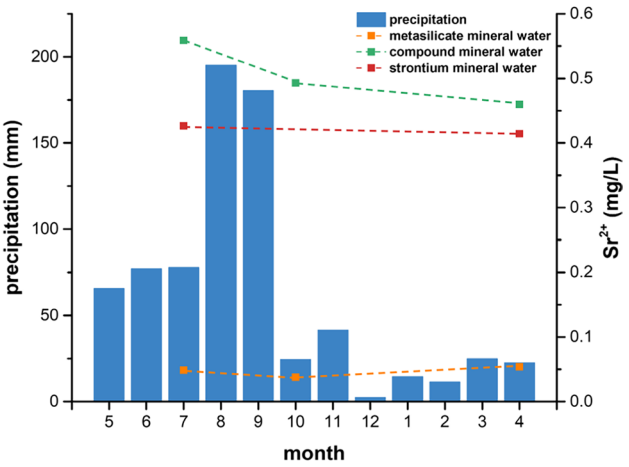

Fig. 11 Relationship between precipitation and Sr^{2+}

for chemical reactions (Bian et al. 2022; Feng et al. 2022). Precipitation is mainly concentrated in July and August (Li et al. 2022). Solute changes in mineral water, especially in the Sr content, had a small range before and after the precipitation and snowmelt periods (Fig. 11), and climate had no significant effect on promoting or weakening rock weathering. However, the study area as a whole was greatly affected by volcanic tectonic movement, and a large number of faults are present. These faults facilitate the movement of water and also provide a good space for water storage, facilitating the full progress of the water-rock reaction (Sun et al. 2019; Tao et al. 2011).

Additionally, CO_2 in atmospheric and soil surfaces can both enter the spring water through precipitation. The soil in the study area was mostly white muddy soil rich in humus, which greatly increased the biological activity in the soil, such that the pCO_2 was considerably higher than the atmospheric level (Shen et al. 2013; Tian et al. 2014). Plant roots secrete organic acids and transpire, which increases the carbonic acid content in the soil and also promotes the weathering of silicate rocks (Berner 1997; Caldeira 2006). Low-molecular-weight organic acids are important intermediates in the process of organic matter metabolism. They are ubiquitous in plants and will enter the soil with the withering of leaves and fruits (Xiao and Wu 2014). The vegetation and forest coverage in the Changbai Mountain area is high, and the soil is mainly albic soil rich in humus, which provides an excellent ecological environment for the enrichment of low molecular weight organic acids. Overall, oxalic acid > propionic acid > tartaric acid > citric acid in the study area (Li 2022). Organic acids can be formed and produced with the growth of vegetation and provide free H^+ in the dissolution process of silicate. The leaching experiments of basalt with different concentrations of oxalic acid solution show that the dissolution of metasilicate increased with the

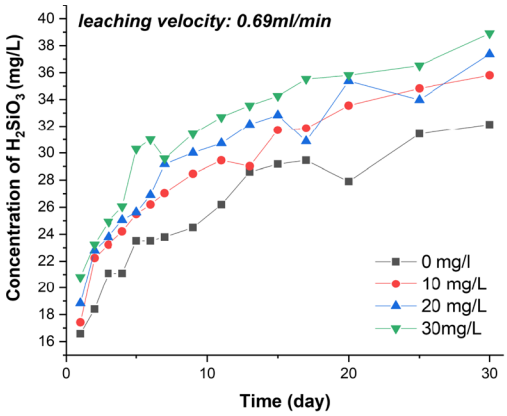

(a) basalt leaching experiment under different concentrations of oxalic acid (Li, 2022)

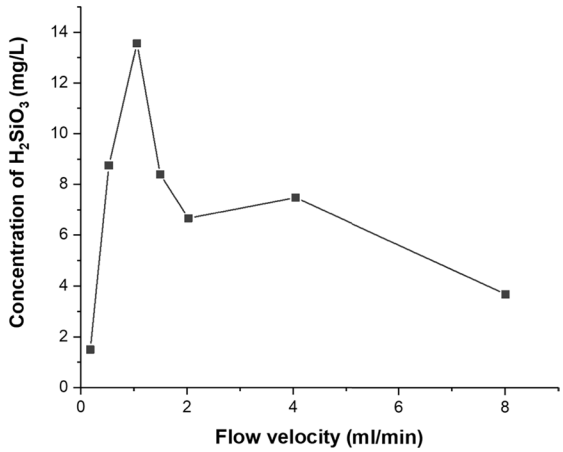

(b) soil leaching experiment under different velocities

Fig. 12 Results of the leaching experiment

increase of acid concentration (Fig. 12a). In the leaching experiment of the surface soil, the content of metasilicate was initially in a rapid upward trend, but when the leaching amount and velocity increased, the soluble substances in the soil decreased continuously, and the concentration of metasilicate decreased (Fig. 12b). These results show that organic acids in soil have an important influence on silicate weathering.

Based on the above analysis, we concluded that the lithological characteristics and the unique high-coverage vegetation environment play a major role in weathering of the Changbai Mountain area. The rock weathering in Changbai Mountain was the supply-limited type.

Conclusions

A combined application of the hydrochemistry method and Sr isotope analysis was employed to investigate the characteristics of different mineral water and rock weathering processes in mountainous basalt areas. The main conclusions are as follows:

(1) According to the hydrochemistry characteristics, mineral water can be divided into three types: metasilicate, strontium, and compound mineral water types. Different types of mineral waters exhibit certain differences. Metasilicate and compound mineral water were mainly of the HCO_3-Mg type, mixed with a small amount of HCO_3-Ca. Moreover, HCO_3-Na also exists in the metasilicate mineral water. Strontium mineral water was of the HCO_3-Ca type.
(2) The solute source of mineral water was dominated by rock weathering. The endmember comparison shows that the isotope composition of metasilicate and compound mineral water was controlled by silicate rocks, whereas the strontium mineral water was mainly controlled by carbonate rocks.
(3) The total dissolution load of rock weathering estimated by stoichiometric equilibrium and chemical flux was

6.76 tons/km^2/year, of which 44.6% and 36.9% were attributed to silicate and carbonate weathering, respectively. The total CO_2 consumption rate was 1.44×10^{10} mol/year. The consumption rates of silicate and carbonate were 8.4×10^9 mol/year and 6.02×10^9 mol/year, respectively. Trace carbonates also played an important role in basalt weathering.

(4) The overall weathering mechanism in the study area was the supply-limited type. The rock composition with pyroxene, feldspar, and olivine as the main minerals determines the internal factors of rock weathering. For external factors, the large area of vegetation coverage and the distribution of humus-rich albic soil contribute to the formation of organic acids, which promotes rock weathering.

Author contribution Yihan Li: methodology, formal analysis, writing—original draft. Jianmin Bian: project administration. Peng Xu: data curation. Xiaoqing Sun: writing—review and editing. Wenhao Sun: data curation.

Funding This work was supported by the National Key R&D Program of China (grant number: 2019YFC0409103) and Graduate Innovation Fund of Jilin University (grant number: 2023CX099).

Data availability Data available on request from the authors.

Declarations

Ethical approval Not applicable.

Consent to participate Not applicable.

Consent for publication Not applicable.

Competing interests The authors declare no competing interests.

References

Aloisi G, Wallmann K, Tishchenko P, Haeckel M, Pavlova G, Greinert J, Eisenhauer A (2006) A possible long-term CO_2 sink through submarine weathering of detrital silicates. Geochim Cosmochim Ac 70(18):A11

Amiri V, Berndtsson R (2020) Fluoride occurrence and human health risk from groundwater use at the west coast of Urmia Lake, Iran. Arab J Geosci 13(18):921

Bello M, Ketchemen-Tandia B, Nlend B, Huneau F, Fouepe A, Fantong WY, Boum-Nkot SN, Garel E, Celle-Jeanton H (2019) Shallow groundwater quality evolution after 20 years of exploitation in the southern Lake Chad: hydrochemistry and stable isotopes survey in the far north of Cameroon. Environ Earth Sci 78(15)

Berner RA (1997) The rise of plants and their effect on weathering and atmospheric CO_2. Science 276(5312):544–546

Berner RA, Maasch KA (1996) Chemical weathering and controls on atmospheric O_2 and CO_2: fundamental principles were enunciated by J.J. Ebelmen in 1845. Geochim Cosmochim Ac 60(9):1633–1637

Bian JM, Li YH, Ma YX, Li JL, Yu YX, Sun WH (2022) Study on hydrochemical characteristics and formation process of Antu mineral water in Changbai Mountain, China. Water-Sui 14(18)

Bickle MJ, Bunbury J, Chapman HJ, Harris NB, Fairchild IJ, Ahmad T (2003) Fluxes of Sr into the headwaters of the Ganges. Geochim Cosmochim Ac 67(14):2567–2584

Blum JD, Gazis CA, Jacobson AD, Page Chamberlain C (1998) Carbonate versus silicate weathering in the Raikhot watershed within the High Himalayan Crystalline Series. Geology 26(5):411–414

Bluth GJS, Kump LR (1994) Lithologic and climatologic controls of river chemistry. Geochim Cosmochim Ac 58(10):2341–2359

Buggle B, Glaser B, Hambach U, Gerasimenko N, Marković S (2011) An evaluation of geochemical weathering indices in loess–paleosol studies. Quat Int 240(1):12–21

Caldeira K (2006) Forests, climate, and silicate rock weathering. J Geochem Explor 88(1-3):419–422

Carol E, Kruse E, Mas-Pla J (2009) Hydrochemical and isotopical evidence of ground water salinization processes on the coastal plain of Samborombon Bay, Argentina. J Hydrol 365(3-4):335–345

Chai Y, Xiao C, Li M, Liang X (2020) Hydrogeochemical characteristics and groundwater quality evaluation based on multivariate statistical analysis. Water-Sui 12(10):2792

Cloutier V (2004) Origin and geochemical evolution of groundwater in the Paleozoic Basses-Laurentides sedimentary rock aquifer system, St. Lawrence Lowlands, Québec, Canada, INRS—Eau. PhD diss., PhD Thesis, INRS-Eau, Terre & Environnement, Québec, Canada

Cloutier V, Lefebvre R, Therrien R, Savard MM (2008) Multivariate statistical analysis of geochemical data as indicative of the hydrogeochemical evolution of groundwater in a sedimentary rock aquifer system. J Hydrol 353(3-4):294–313

Clow DW, Mast MA, Bullen TD, Turk JT (1997) Strontium 87/strontium 86 as a tracer of mineral weathering reactions and calcium sources in an Alpine/Subalpine Watershed, Loch Vale. Colorado Water Resour Res 33(6):1335–1351

Dalai TK, Krishnaswami S, Kumar A (2003) Sr and 87Sr/86Sr in the Yamuna River System in the Himalaya: sources, fluxes, and controls on Sr isotope composition. Geochim Cosmochim Ac 67(16):2931–2948

Dessert C, Dupré B, Gaillardet J, François LM, Allègre CJ (2003) Basalt weathering laws and the impact of basalt weathering on the global carbon cycle. Chem Geol 202(3-4):257–273

Deuerling KM, Martin JB, Martin EE, Scribner CA (2018) Hydrologic exchange and chemical weathering in a proglacial watershed near Kangerlussuaq, west Greenland. J Hydrol 556:220–232

Dinelli E, Lima A, De Vivo B, Albanese S, Cicchella D, Valera P (2010) Hydrogeochemical analysis on Italian bottled mineral waters: Effects of geology. J Geochem Explor No.3:317–335

Dixon JL, Hartshorn AS, Heimsath AM, DiBiase RA, Whipple KX (2012) Chemical weathering response to tectonic forcing: a soils perspective from the San Gabriel Mountains, California. Earth Planet Sc Lett 323:40–49

Elena FEFY, Vasiliy L, Natalia K, Arslan S, Elena M, Ekaterina B, Anna K, Alexey M, Elena B (2020) Hydrogeology and hydrogeochemistry of mineral sparkling groundwater within Essentuki area (Caucasian mineral water region). Environ Earth Sci No.1:1–12

Ettayfi N, Bouchaou L, Michelot JL, Tagma T, Warner N, Boutaleb S, Massault M, Lgourna Z, Vengosh A (2012) Geochemical and isotopic (oxygen, hydrogen, carbon, strontium) constraints for the origin, salinity, and residence time of groundwater from a carbonate aquifer in the Western Anti-Atlas Mountains, Morocco. J Hydrol 438-439:97–111

Fan B, Zhao Z, Tao F, Liu B, Tao Z, Gao S, Zhang L (2014) Characteristics of carbonate, evaporite and silicate weathering in Huanghe

River basin: a comparison among the upstream, midstream and downstream. J Asian Earth Sci 96:17–26
Feng M, Zhang W, Zhang S, Sun Z, Li Y, Huang Y, Wang W, Qi P, Zou Y, Jiang M (2022) The role of snowmelt discharge to runoff of an alpine watershed: evidence from water stable isotopes. J Hydrol 604:127209
Fillimonova E, Kharitonova N, Baranovskaya E, Aseeva AMA (2022) Geochemistry and therapeutic properties of Caucasian mineral waters: a review. Environ Geochem Hlth No.7:2281–2299
Fu H, Jian X, Liang H, Zhang W, Shen X, Wang L (2022) Tectonic and climatic forcing of chemical weathering intensity in the northeastern Tibetan Plateau since the middle Miocene. Catena 208:105785
Gabet EJ, Mudd SM (2009) A theoretical model coupling chemical weathering rates with denudation rates. Geology 37(2):151–154
Gaillardet J, Dupre B, Louvat P, Allegre CJ, Probst J, Faure H, Veizer J (1999) Global silicate weathering and CO (sub 2) consumption rates deduced from the chemistry of large rivers. Chem Geol 159(1-4):3–30
Garzanti E, Padoan M, Andò S, Resentini A, Vezzoli G, Lustrino M (2013) Weathering and relative durability of detrital minerals in equatorial climate: sand petrology and geochemistry in the East African Rift. J Geol 121(6):547–580
Garzanti E, Padoan M, Setti M, López-Galindo A, Villa IM (2014) Provenance versus weathering control on the composition of tropical river mud (southern Africa). Chem Geol 366:61–74
Gibbs RJ (1970) Mechanisms controlling world water chemistry. Science 170(3962):1088–1090
Guo WF, Liu JQ, Guo ZF (2014) Temporal variations and petrogenetic implications in Changbai basaltic rocks since the Pliocene. Acta Petrol Sin 30(12):3595–3611
Han G, Liu C (2004) Water geochemistry controlled by carbonate dissolution: a study of the river waters draining karst-dominated terrain, Guizhou Province, China. Chem Geol 204(1-2):1–21
Horton TW, Chamberlain CP, Fantle M, Blum JD (1999) Chemical weathering and lithologic controls of water chemistry in a high-elevation river system: Clark's Fork of the Yellowstone River, Wyoming and Montana. Water Resour Res 35(5):1643–1655
Jiang H, Lee CA (2019) On the role of chemical weathering of continental arcs in long-term climate regulation: a case study of the Peninsular Ranges batholith, California (USA). Earth Planet Sci Lett 525:115733
Kump LR, Brantley SL, Arthur MA (2000) Chemical, weathering, atmospheric CO_2, and climate. Annu Rev Earth Pl Sci 28:611–667
Lambrakis N, Antonakos A, Panagopoulos G (2004) The use of multicomponent statistical analysis in hydrogeological environmental research. Water Res 38(7):1862–1872
Lavrushin VY, Israfailov YG, Polyak BG, Pokrovsky BG, Bujakaite MI, Kamensky IL (2018) Conditions of the formation of thermomineral waters in the Talysh Fold Zone of the Lesser Caucasus (Azerbaijan) based on isotope-geochemical data ($^3He/^4He$, $\delta^{13}C_{CO2}$, $\delta^{13}C_{CH4}$, $\delta^{15}N_{N2}$, $^{87}Sr/^{86}Sr$, δD_{H2O}, and $\delta^{18}O_{H2O}$). Lithol Miner Resour No.1:53–75
Li D (2022) Genesis of metasilicate mineral water in the basalt area, Changbai Mountain: an experimental study on the kinetics of the water-rock interactions. Master Jilin University
Li X, Han G, Liu M, Yang K, Liu J (2019) Hydro-geochemistry of the river water in the Jiulongjiang River Basin, Southeast China: implications of anthropogenic inputs and chemical weathering. Int J Environ Res Public Health 16(3):440
Li Y, Bian J, Li J, Ma Y, Anguiano JHH (2022) Hydrochemistry and stable isotope indication of natural mineral water in Changbai Mountain, China. J Hydrol Reg Stud 40:101047
Liu Z, Dreybrodt W, Liu H (2011) Atmospheric CO_2 sink: silicate weathering or carbonate weathering? Appl Geochem 26:S292–S294
Ma H, Yang Q, Pan X, Wu C, Chen C (2015) Origin of Early Pleistocene basaltic lavas in the Erdaobaibe River basin, Changbaishan region. Acta P etrologica Sinica 31(11):3484–3494
Maher K, Chamberlain CP (2014) Hydrologic regulation of chemical weathering and the geologic carbon cycle. Science 343(6178):1502–1504
Marandi A, Shand P (2018) Groundwater chemistry and the Gibbs diagram. Appl Geochem 97:209–212
Meybeck M (1987) Global chemical weathering of surficial rocks estimated from river dissolved loads. Am J Sci 287(5):401
Moon S, Huh Y, Qin J, van Pho N (2007) Chemical weathering in the Hong (Red) River basin: rates of silicate weathering and their controlling factors. Geochim Cosmochim Ac 71(6):1411–1430
Negrel P, Casanova J, Blomqvist R, Kaija J, Frape S (2003) Strontium isotopic characterization of the Palmottu hydrosystem (Finland): water-rock interaction and geochemistry of groundwaters. Geofluids 3(3):161–175
Negrel P, Pauwels H (2004) Interaction between different groundwaters in Brittany catchments (France): characterizing multiple sources through strontium- and sulphur isotope tracing. Water Air Soil Pollut 151(1-4):261–285
Negrel P, Pauwels H, Chabaux F (2018) Characterizing multiple water-rock interactions in the critical zone through Sr-isotope tracing of surface and groundwater. Appl Geochem 93:102–112
Nesbitt HW, Young GM, McLennan SM, Keays RR (1996) Effects of chemical weathering and sorting on the petrogenesis of siliciclastic sediments, with implications for provenance studies. J Geol 104(5):525–542
Oliva P, Viers J, Dupre B (2003) Chemical weathering in granitic environments. Chem Geol 202(3-4):225–256
Pang H, Pan B, Garzanti E, Gao H, Zhao X, Chen D (2018) Mineralogy and geochemistry of modern Yellow River sediments: implications for weathering and provenance. Chem Geol 488:76–86
Panno SV, Kelly WR, Askari Z, Hackley KC, Krothe J (2022) Stratigraphic and structural controls on the occurrence of saline springs within the Illinois Basin, U.S. J Hydrol 610:127823
Paytan A, Griffith EM, Eisenhauer A, Hain MP, Wallmann K, Ridgwell A (2021) A 35-million-year record of seawater stable Sr isotopes reveals a fluctuating global carbon cycle. Science 371(6536):1346–1350
Riebe CS, Hahm WJ, Brantley SL (2017) Controls on deep critical zone architecture: a historical review and four testable hypotheses. Earth Surf Process Landf 42(1):128–156
Riebe CS, Kirchner JW, Finkel RC (2004) Erosional and climatic effects on long-term chemical weathering rates in granitic landscapes spanning diverse climate regimes. Earth Planet Sc Lett 224(3-4):547–562
Roy S, Gaillardet J, Allègre CJ (1999) Geochemistry of dissolved and suspended loads of the Seine River, France: anthropogenic impact, carbonate and silicate weathering. Geochim Cosmochim Ac 63(9):1277–1292
Ryu JS, Lee KS, Chang HW (2007) Hydrogeochemical and isotopic investigations of the Han River Basin, South Korea. J Hydrol 345(1-2):50–60
Santoni S, Huneau F, Garel E, Aquilina L, Vergnaud-Ayraud V, Labasque T, Celle-Jeanton H (2016) Strontium isotopes as tracers of water-rocks interactions, mixing processes and residence time indicator of groundwater within the granite-carbonate coastal-aquifer of Bonifacio (Corsica, France). Sci Total Environ 573:233–246
Shand, P., Darbyshire, DPF, Love, AJ, & Edmunds, WM. (2009). Sr isotopes in natural waters: Applications to source characterisation and water–rock interaction in contrasting landscapes. Appl Geochem, 24(4), 574-586.

Shen C, Xiong J, Zhang H, Feng Y, Lin X, Li X, Liang W, Chu H (2013) Soil pH drives the spatial distribution of bacterial communities along elevation on Changbai Mountain. Soil Biol Biochem 57:204–211

Shi D, Tan H, Chen X, Rao W, Basang R (2021) Uncovering the mechanisms of seasonal river–groundwater circulation using isotopes and water chemistry in the middle reaches of the Yarlungzangbo River. Tibet J Hydrol 603:127010

Spence J, Telmer K (2005) The role of sulfur in chemical weathering and atmospheric CO_2 fluxes: evidence from major ions, delta C-^{13}(DIC), and delta S-^{34}(SO_4) in rivers of the Canadian Cordillera. Geochim Cosmochim Ac 69(23):5441–5458

Spence J, Telmer K (2006) The role of sulfur in chemical weathering and atmospheric CO_2 fluxes: evidence from major ions, $\delta^{13}C_{DIC}$, and $\delta^{34}S_{SO4}$ in rivers of the Canadian Cordillera. Geochim Cosmochim Ac No.23:5441–5458

Suchet PA, Probst JL (1995) A global model for present-day atmospheric/soil CO_2 consumption by chemical erosion of continental rocks (GEM-CO_2). Tellus B 47(1-2):273–280

Sun M, Wu W, Ji X, Wang X, Qu S (2019) Silicate weathering rate and its controlling factors: a study from small granitic watersheds in the Jiuhua Mountains. Chem Geol 504:253–266

Tao Z, Gao QZ, Wang ZG, Zhang SH, Xie CJ, Lin PS, Ruan XB, Li SH, Mao HR (2011) Estimation of carbon sinks in chemical weathering in a humid subtropical mountainous basin. Chin Sci Bull 56(35):3774–3782

Tian M, Wang Z, Bai R, Sun C, Wang D (2014) Geochemistry of pedogenesis of dark brown soil in Changbai Mountain area. Glob Geol 3:695–701

Toth J (1999) Groundwater as a geologic agent: an overview of the causes, processes, and manifestations. Hydrogeol J 7(1):1–14

van der Aa M (2003) Classification of mineral water types and comparison with drinking water standards. Environ Geol 44(5):554–563

Vaughn, B.H., Fountain, A.G., 2005. MacAyeal, D.R. (ed), pp. 107-112, International symposium on ice and water interactions.

Wang G, Xiao C, Qi Z, Lai Q, Meng F, Liang X (2021b) Research on the exploitation and utilization degree of mineral water based on ecological base flow in the Changbai Mountain basalt area, northeast China. Environ Geochem Hlth.

Wang RF, Wu X, Zhai YL, Su YX, Liu CH (2021a) An experimental study on the sources of strontium in mineral water and general rules of its dissolution-a case study of Chengde. Hebei Water-Sui 13(5)

Wang Y, Guo Q, Su C, Ma T (2006) Strontium isotope characterization and major ion geochemistry of karst water flow, Shentou, northern China. J Hydrol 328(3-4):592–603

Wimpenny J, Yin Q, Tollstrup D, Xie L, Sun J (2014) Using Mg isotope ratios to trace Cenozoic weathering changes: a case study from the Chinese Loess Plateau. Chem Geol 376:31–43

Wu W, Zheng H, Yang J, Luo C, Zhou B (2013) Chemical weathering, atmospheric CO_2 consumption, and the controlling factors in a subtropical metamorphic-hosted watershed. Chem Geol 356:141–150

Wu Y, Luo Z, Luo W, Ma T, Wang Y (2018) Multiple isotope geochemistry and hydrochemical monitoring of karst water in a rapidly urbanized region. J Contam Hydrol 218:44–58

Wu Y, Wang Y (2014) Geochemical evolution of groundwater salinity at basin scale: a case study from Datong basin, Northern China. Environ Sci Process Impacts 16(6):1469–1479

Xiao M, Wu F (2014) A review of environmental characteristics and effects of low-molecular weight organic acids in the surface ecosystem. J Environ Sci-China 26(5):935–954

Yan B, Qiu S, Xiao C, Liang X (2019) Characteristics of mineral fluids and geothermal reservoir in Changbai Mountain, northeast of China. Geochem Int 57(1):83–97

Yan B, Xiao C, Liang X, Wei R, Wu S (2015) Characteristics and genesis of mineral water from Changbai Mountain, Northeast China. Environ Earth Sci 73(8):4819–4829

Yan B, Xiao C, Liang X, Wu S (2016) Hydrogeochemical tracing of mineral water in Jingyu County, Northeast China. Environ Geochem Hlth 38(1):291–307

Yan B, Xiao C, Liang X, Wu S (2017) Influences of pH and CO_2 on the formation of metasilicate mineral water in Changbai Mountain, Northeast China. Appl Water Sci 7(4):1657–1667

Zeng Q, Liu Z (2017) Is basalt weathering a major mechanism for atmospheric CO_2 consumption? Chin Sci Bull 62(10):1041–1049

Zhang H, Wu Y, Luo W, Chen W, Liu H (2020) Hydrogeochemical investigations of groundwater in the Lingbei area, Leizhou Peninsula. Huan jing ke xue= Huanjing kexue 41(11):4924–4935

Zhang S, Han G, Zeng J, Xiao X, Malem F (2021) A strontium and hydro-geochemical perspective on human impacted tributary of the Mekong River Basin: sources identification, fluxes, and CO_2 consumption. Water-Sui 13(21):3137

Zhang X, Xu Z, Liu W, Moon S, Zhao T, Zhou X, Zhang J, Wu Y, Jiang H, Zhou L (2019) Hydro-geochemical and Sr isotope characteristics of the Yalong River Basin, Eastern Tibetan Plateau: implications for chemical weathering and controlling factors. Geochem Geophys Geosyst 20(3):1221–1239

Zhao R, Shan X, Wu C, Yi J, Hao G, Wang P (2019) Formation and evolution of the Changbaishan volcanic geothermal system in a convergent plate boundary back-arc region constrained by boron isotope and gas data. J Hydrol 569:188–202

Zhao R, Yi J (2021) Geochemistry of thermal waters in the Changbaishan volcanic geothermal system, Northeast China—implications for vapor-liquid separation controls on geothermal fluid composition. Arab J Geosci 14(6):419

Zhou Z, Jiang C, Li B (1998) Geochemical features of Sr, Nd and Pb isotopes of volcanic rocks in Cenozoic era in Tengchong, Changbaishan and Wudalianchi, China. J Seismol Res 21:89–97